Kathekeyan, Myuran & Mahendran, Mahen
(2017)
New test and design methods for steel roof battens subject to fatigue pull-through failures.
Thin-Walled Structures, *119*, pp. 558-571.

https://doi.org/10.1016/j.tws.2017.07.007

NEW TEST AND DESIGN METHODS FOR STEEL ROOF BATTENS SUBJECT TO FATIGUE PULL-THROUGH FAILURES

Kathekeyan Myuran and Mahen Mahendran

Queensland University of Technology (QUT), Brisbane, Australia.

Abstract: Thin steel roof claddings and battens are widely used in low rise buildings all around the world. However, they are vulnerable to premature connection failures when subjected to severe wind uplift actions such as those induced by cyclones and storms. Current design methods exclusively depend on full scale prototype roof tests. This paper proposes an alternative design method using a simple equation for thin-walled steel roof battens subjected to fatigue pull-through failures, developed through a series of small scale cyclic wind load tests of roof battens. Since an acceptable small scale connection test method is not available for fatigue pull-through failures of roof battens, various types of small scale connection tests were initially examined to propose the most suitable test method. For this purpose, a series of constant amplitude cyclic tests was conducted using three different small scale test methods (short, cantilever and two-span battens), for a commonly used steel roof batten. Test results showed that the present state of knowledge based on static pull-through studies could lead to the use of a wrong test method in fatigue pull-through studies. This paper has used the cyclic test results from the selected small scale test method to propose a fatigue pull-through design equation. The use of the proposed design equation will lead to conservative outcomes for roof battens and will enable safe roof batten design without the need for full scale cyclic tests of prototype roof assemblies.

Keywords: Cold-formed steel roof battens; Cyclic wind uplift action; Pull-through failures; Experimental study; Fatigue; Small scale test methods; Design equations.

Corresponding author’s email address: m.mahendran@qut.edu.au

1 INTRODUCTION

Low-pitched roofs made of light gauge steel roof claddings and battens are vulnerable to premature pull-through failures during severe wind events such as cyclones and storms. Figure 1 shows the two critical connections in a steel roof that are susceptible to pull-through failures. The first is the cladding to batten connection which connects the roof cladding to batten and the second is the batten to rafter/truss connection which connects the roof batten to rafter/truss in a building. The wind uplift load on the roof cladding is first transferred to battens via cladding to batten connections and then to rafter/truss via batten to rafter connections. As the cladding and battens are made of thin, high strength steel with low ductility, their connections are likely to fail under cyclic wind uplift loading due to pull-through failures. Post-cyclone investigations and past research studies have revealed that low cycle fatigue cracking around the screw fastener holes is the reason for the pull-through failures [1, 2], and the possibility of such fatigue pull-through failures is high in a low-pitch low-rise building roof near the eaves and ridges where the suction wind pressure is extremely high [3].

In the past, fatigue pull-through failures were limited to cladding to batten connections as shown in Figure 2(a). It occurs when the cyclic wind uplift loading creates radial fatigue cracks in the roof cladding around the fastener holes, allowing the screw fastener to pull through the roof cladding. Many research studies [4-6] have investigated the fatigue pull-through failures of cladding to batten connections and improved the roof design to overcome the fatigue pull-through failure. Due to such improvements, fatigue pull-through failures have now moved to the next weakest connection, i.e. batten to rafter/truss connection [7]. A wind tunnel study conducted by Ginger [8] also confirmed that not only the cladding to batten connections, but also the batten to rafter/truss connections experience the same kind of cyclic wind uplift loading and thereby prone to fatigue pull-through failures. Therefore, this paper focuses on the premature fatigue pull-through failures in the vicinity of batten to rafter/truss connections.

The fatigue pull-through failures in the batten to rafter connections occur when the cyclic wind uplift loading generates fatigue cracks around the batten to rafter screw heads and lets the screw fasteners to pull through both bottom flanges of the roof batten as shown in Figure 2(b). Although the batten pull-through failure is similar to the cladding pull-through failure, the failure mode is different since the cladding pull-through failure is typically due to severe cracking of cladding originating from the screw hole whereas the batten pull-through failure is due to tearing around the screw head [9]. Due to this difference, the design and test methods/guidelines developed for the cladding to batten connection pull-through failure cannot be used for batten to rafter connection pull-through failures [10]. Considering this, Sivapathasundaram and Mahendran [10, 11] developed new design equations to determine the static pull-through capacities of cold-formed steel roof battens. However, they did not consider the effects of cyclic wind loading and the resulting fatigue pull-through failures. Currently available design capacity tables provided by the roof batten manufacturers also do not specify the static and fatigue pull-through failure capacities.

Due to the unavailability of fatigue pull-through capacity design equations for roof battens, the current design method depends entirely on large scale prototype roof testing based on a Low-High-Low (LHL) cyclic loading sequence recommended by the National Construction Code of Australia (NCC) [12]. Prototype roof panels must be tested to a design cyclone which is simulated by the multi-level fatigue loading sequence such as the LHL loading sequence as suggested by Mahendran [13]. The roof assemblies must be tested by including roof cladding, its immediate supporting members such as roof batten and rafter and their connections. Besides, the test should be repeated multiple times, considering the variability of structural components. Therefore, it is desirable to eliminate this complex, expensive and time consuming LHL prototype testing by developing a simple fatigue design equation and/or a small scale isolated connection test method. However, a standard test method or set-up is not available to conduct such small scale isolated connection tests that are suitable for assessing the fatigue pull-through capacities of steel roof battens. The test method proposed by Sivapathasundaram and Mahendran [9] to conduct the static pull-through failure studies may not be suitable for fatigue pull-through failure studies as the failure modes and the wind actions that cause the failures are different.

Therefore, as the first step of developing a suitable design equation for the fatigue pull-through failure of roof battens, this study initially focused on determining a suitable small scale test method that simulates the fatigue pull-through failures of batten to rafter connections by considering all the influential factors. For this purpose, 0.75 mm thick G550 steel (minimum tensile strength of 550 MPa) industrial roof battens (G550-0.75 batten) were used (Figure 3). The study then focused on developing a simple design equation to determine the fatigue life of the G550-0.75 battens by means of a cyclic test series conducted using the selected small scale test method. In the past, a fatigue life approach based only on the applied cyclic load magnitude was used for this purpose. Beck and Stevens [14] was the first who used such an approach to investigate the fatigue behaviour of steel roof cladding. They used a series of constant amplitude cyclic loading tests and produced a cyclic load amplitude versus fatigue life (number of cycles to failure) curve, which is commonly known as the S-N curve to predict the fatigue capacity. A similar approach was then used by Mahendran [4], Xu [5] and Mahendran and Mahaarachchi [15] to determine the fatigue capacities of cladding to batten connection failures. The same fatigue life approach was used in this study to investigate the fatigue behaviour of the G550-0.75 battens and determine their fatigue life. Finally, the static pull-through capacity equation developed by Sivapathasundaram and Mahendran [10, 11] was modified to design the G550-0.75 battens for fatigue pull-through failures without conducting any large scale prototype LHL tests.

2 EXPERIMENTAL STUDY

An experimental study was designed to select a suitable small scale test method and thereby develop a simple fatigue pull-through capacity equation. For this purpose, a suitable small scale test should be developed by considering all the factors that affect the fatigue pull-through behaviour of roof battens. Besides, in order to verify its suitability, it should be compared with the results from a full scale test which simulates the actual fatigue pull-through failure of roof battens. According to NCC [12], a large scale prototype roof assembly can be used to simulate roof failures. AS 4040.3 [16], on the other hand, recommends at least a two-span roof assembly to simulate multi-span roof assemblies. Therefore, considering both NCC [12] and AS 4040.3 [16] guidelines, a two-span prototype roof assembly was considered adequate to simulate the pull-through failures of roof battens, and was used to verify the suitability of the small scale test method. Also, the two-span prototype roof tests (hereinafter referred to as full scale tests) would highlight the difficulties in conducting LHL tests. Hence, initially, full scale roof assemblies of dimensions 2.4 m x 1.5 m were tested to investigate the actual fatigue pull-through behaviour, fatigue life and failure patterns of roof battens. Then, a series of three different small scale test methods using short (150 mm long batten), cantilever (500 mm long batten) and two-span battens (1800 mm long batten) was included. The most suitable small scale test method was then selected by comparing the test results with the full scale test results. Finally, the selected small scale test method was used to develop a simple design equation. Considering the fatigue life approach, all the full scale and small scale tests were conducted under constant amplitude cyclic loading. The cyclic loading was maintained in the form of a sine wave with a positive mean load and a positive load ratio. A 0.75 mm thick hat shaped batten made of G550 steel (minimum tensile strength of 550 MPa) (Figure 3) was used throughout the test series with 10 gauge Teks screws.

2.1 Full Scale Tests

Two-span roof panels of dimensions 2.4 m x 1.5 m were made using commonly used roof components. However, careful attention was given in selecting each roof component as a poor selection could lead to other types of failures such as pull-out and local dimpling. A thicker corrugated steel roof cladding with 0.48 mm BMT was selected to avoid local dimpling failures of roof sheeting. Likewise, a 3 mm thick lipped channel was chosen as the rafter to reduce the flexibility effect of rafters, i.e. to prevent outward flange deformations of the lipped channel and thereby eliminating any prying forces on the screw fasteners. Figures 4(a) and (b) show the roof cladding, three roof battens and three rafters used in the full scale two-span roof assembly. As shown in Figure 4(a), the roof battens were used at 750 mm spacing with a span of 1200 mm to represent realistic batten configuration, while avoiding member failures of roof battens. Currently available batten design capacity tables [17] were used for this purpose. Roof cladding was alternate crest-fixed to battens using 6.5 x 55 roofing zips with cyclone washers to avoid pull-through failure in the roof cladding to batten connections. In order to avoid twisting of roof battens, special attention was given during the drilling process to ensure all roofing screws were drilled vertically through the centre of batten's top flange. A specially made jig was used to drill the holes in the bottom flanges of the test battens to maintain consistency among tests and to maintain symmetry of test battens. 10 gauge (10g) metal Teks screws were used to fix the battens to the lipped channel rafters. To prevent pull-out failures at the critical central batten to rafter connection in the middle roof batten, nuts and bolts were used instead of 10g metal Teks screws. Special washers (made from 10g Teks screw head) were used along with bolts to simulate the actual Teks screw-batten connection as shown in Figure 4(c). Lock nuts were used to prevent the loosening of bolts during cyclic tests.

The full scale two-span roof assembly was then located in the air-box as shown in Figure 4(b) with rafters on the top, and tested by subjecting the roof sheeting to a wind suction pressure using an air pump. Clark rubber seal was used along the edges of the full scale roof panels whilst an adhesive tape was used along cladding joints to prevent air leakage. Initially, a series of static tests, was conducted to determine the static pull-through capacity, which sets the upper bound of the roof batten's S-N curve. The suction pressure inside the air-box was slowly increased until the critical central batten to rafter bolt/screw head completely pulled through the batten's bottom flanges. The loading was increased at a very slow rate (less than 1 kN/min), as recommended by the American Iron and Steel Institute (AISI) standard for the test method of mechanically fastened CFS connections [18]. The load transferred to the critical central batten to rafter connection was measured by recording the bolt reaction forces using two 15 kN washer load cells as shown in Figure 4(d).

Then a series of constant amplitude cyclic load tests was conducted with cyclic load ranges (equal to the maximum cyclic loads since the minimum cyclic load was about zero) equal to different percentages (40 to 100%) of the roof batten's measured mean static pull-through failure capacity to determine the fatigue life (number of cycles to failure), and thereby produce the S-N curve. The constant amplitude cyclic load was maintained at 1 Hz sinusoidal wave form by two cyclic valves and a controller (Figure 4(b)). Besides, for each test, the required pressure inside the air-box was adjusted based on the load cell reading. In order to record the 1 Hz sinusoidal waveform, test data were recorded at a sample rate of 10 Hz. A typical cyclic load variation with the maximum cyclic load equal to 50% of the batten's mean static pull-through capacity (hereinafter referred to as 50% cyclic test) is shown in Figure 4(e).

2.2 Small Scale Isolated Connection Tests

Many past studies [9, 19, 20] have used small scale isolated connection tests to investigate the roof failures since they are localised to the connection regions. Therefore, considering the small scale tests used in the past, three different small scale tests were included, namely, short (150 mm long batten), cantilever (500 mm long batten) and two-span (1800 mm long batten) batten tests.

2.2.1 Short batten tests

Since the pull-through failures are limited to connection regions, a 150 mm long short batten was selected as the first small scale test method and tested using a 100 kN mechanical testing system (MTS) (Figure 5). In this test method, the load is applied to the top flange of the batten, directly below the two bottom flange connections. Despite the fact that the actual batten's bending action cannot be simulated in the short batten, it was included in the test series as it is the recommended test method for static pull-through studies of roof battens [9]. Besides, it will help to investigate the absence of bending effect on the fatigue pull-through failures. Similar to air-box tests, both static and cyclic tests were conducted to obtain the S-N curve. A testware with user created procedures was used to operate the MTS. The procedures were created using a sequence of commands to apply the load, record data and to stop the test automatically when the failure occurs. The static loading was applied in displacement control mode at a rate of 1mm/min, whereas cyclic tests were applied in load control mode at a frequency of 1 Hz. The fatigue life of the test batten (number of cycles to failure) was recorded automatically and obtained from the MTS testware. In order to investigate the crack initiation and the behaviour of the batten during the cyclic test, displacement was measured at the top flange of the batten, where the load was applied.

2.2.2 Cantilever batten tests

The roof battens are subjected to a bending action along their length while their screw fasteners are subjected to a tensile load under wind uplift loading. Their pull-through failures occur under these two actions. Therefore, to include the effect of bending, a cantilever batten with an overhang length of 240 mm was selected and tested in the MTS (Figure 6). This cantilever length was chosen to simulate the same tension and bending actions in the full scale test based on simple calculations using bending theory. As shown in Figure 6, loading arms were attached to roof batten ends, ensuring the cantilever length of 240 mm. The loads transferred to the batten connections were recorded using the 15 kN washer load cells. Similar to the full scale and short batten tests, a few static tests were first conducted, followed by a series of cyclic tests.

2.2.3 Two-span batten tests

When a connection fails in a multi-span roof assembly, the load carried by the failed connection will be shared by adjacent screw connections. Such load sharing could influence the batten behaviour from the point of fatigue crack initiation. To investigate this, a 1900 mm long two-span batten (900 mm span) was used in the third small scale test method. The span length was calculated using simple bending theory calculations to simulate the actual tension and bending actions in the air-box test with a uniform pressure loading. As shown in Figure 7, roof batten was supported at three locations and the two loading arms were attached to roof batten’s top flange at mid-spans. Cyclic loads were applied by a hydraulic actuator in a sine wave form at 1 Hz as applied in short and cantilever batten tests. The loads transferred to the middle support screws were recorded using two 15 kN washer load cells (Figure 7), and the number of cycles to failure and the mid-span deflections of roof batten were recorded.

3 DISCUSSION OF TEST RESULTS

Table 1 presents the results of the series of static tests. It shows that the static pull-through capacities from all the small scale tests agree reasonably well with the full scale test results and thus small scale tests can be used to determine the static pull-through capacities of roof battens. This agrees with the finding in [9]. The higher test variation (COV = 0.1) noticed in the air-box tests is possibility due to the complex test arrangements. The mean static pull-through capacity obtained from each test method was used to determine the maximum cyclic load required for the constant amplitude cyclic tests conducted using the same test method. Tables 2 to 5 present the number of cycles to failure as a function of the ratio of the maximum cyclic load to the static pull-through capacity expressed as a percentage. Since the minimum cyclic load is about zero, the maximum cyclic load and the cyclic load amplitude are the same.

In fatigue studies, it is preferable to consider crack initiation and propagation separately. However, defining the exact crack initiation point is very difficult. Techniques such as microscopic observation of grain boundaries are frequently used to define the exact crack initiation point. However, in this study, the variation in the recorded batten deformation was used to define the crack initiation point. Figure 8 illustrates the two distinct phases of batten fatigue behaviour. The first one is up to 4400 cycles, below which the displacement increases at a very slow rate because of cyclic ratcheting. This point is defined as the crack initiation (N_i) point after which deformation increases at a higher rate until 6641 cycles when the crack reaches a critical crack length allowing a complete pull-through failure (N_f). The second sudden increment in the displacement between N_i and N_f is due to the crack initiation on the other side of the batten. Although the exact point of invisible microcrack nucleation cannot be determined using this procedure, the point where the batten's behaviour changes can be determined exactly. The number of cycles to crack initiation point (N_i) was obtained for each cyclic test and the results are presented in Tables 3 to 5.

3.1 Full scale air-box tests

As seen in Table 2, the fatigue life (number of cycles to failure) of roof battens increases with decreasing cyclic load amplitude (or maximum cyclic load) until the endurance limit is reached. This can be clearly seen in the S-N curve shown in Figure 9. A significant difference is observed in the batten's behaviour between 40 and 50% cyclic loads. In this region, the number of cycles to failure increases rapidly with decreasing cyclic load amplitude until the batten's endurance limit is reached. Endurance limit is the limiting stress below which a fatigue failure does not occur irrespective of the number of cycles. It shows that the batten's endurance limit is closer to 40% of the batten's static pull-through capacity (hereinafter referred to as 40% SPC).

Another observation noted in the constant amplitude cyclic tests is that the air-box test A-1 (Table 2) with a maximum cyclic load equal to the mean static pull-through capacity (100% SPC) took 635 cycles to reach failure, not one cycle as expected. This unexpected observation is possibly due to the strain rate sensitivity of cold-formed steels. The static tests were conducted at 1 mm/ min quasi-static loading rate, whereas the cyclic tests were conducted at 1 Hz dynamic loading, which is much faster than the static test. The batten's SPC was shown to be directly proportional to the ultimate tensile strength of steel [9] while the ultimate tensile strength of most steels increases with increasing loading/ strain rate [21, 22]. This is because the increasing strain rate decreases the movement of free dislocations by forming mechanical twins (formation of crystal structures) [23]. In other words, it decreases the molecular mobility by making the molecular bonds stiffer. This is the reason for the high number of cycles to failure in Test A-1.

In order to understand the behaviour of roof battens, the load transferred to the screw connections was obtained by measuring the individual screw fastener reaction using washer load cells. Figure 10 shows the fastener reaction versus number of cycles curve obtained from the air-box test A-3 (right hand side - RHS and left hand side - LHS). In an ideal situation, the load transferred from the batten to rafter is equally distributed via batten's two bottom flange screw fasteners. However, in reality, it is not true, especially due to poor cladding to batten screw fastener locations. In a roofing system, wind load on roof cladding is transferred to battens via the cladding to batten screw fasteners. Screw fastening through cladding to batten from the top is difficult, without seeing the exact batten location. This leads to inaccurately located screws on the batten's top flange and inclined screws. This leads to twisting of the batten (Figure 11(a)) and unequal load distribution, resulting in unequal fastener reactions. For carefully fabricated roof assemblies, this unequal load distribution is insignificant and the difference between the fastener reactions is small until failure as shown in Figure 10. To obtain such a perfect load distribution in all the test roof assemblies, roof cladding to batten fasteners were fastened along a pre-drawn line to perfectly locate the batten (Figure 11(b)). However, such a perfect outcome is difficult to achieve in all cases.

Figure 12(a) shows a typical unequal load distribution. Unlike in Figure 10, the reaction force on the RHS screw fastener is much higher (about 33 to 50%) than that on the LHS screw fastener. Moreover, this increased fastener reaction on the RHS screw remains until about 17,500 cycles which is almost 90% of the batten's fatigue life. This damages the RHS screw connection more severely than the LHS screw connection and consequently decreases the fatigue life of the batten by prematurely pulling through on the RHS. This can also be clearly seen in the batten's fatigue pull-through failure modes (Figure 12(b)). Failure modes observed in all the air-box tests are shown in Figure 13. The LHS failure mode shown in Figure 12(b) is similar to the failure mode observed in the air-box static test (Figure 13(a)). This is because of the sudden increase in the load on the LHS after the failure in the RHS (Figure 12(a)), which prematurely pulls through the LHS screw connection (in static pull-through failure mode). This confirms that the unequal load distribution due to poor cladding to batten screw fastening accelerates the fatigue pull-through failure.

In summary, despite the fact that the full scale air-box test provides the best representation of roof assemblies, it has practical difficulties in conducting the fatigue pull-through studies. Therefore, isolated small scale connection tests were preferred in the fatigue pull-through studies.

3.2 Small scale tests

Initially, the short batten test results were compared with the full scale air-box test results to verify the suitability of the short batten test (see Figure 14). As seen in Figure 14, the S-N curve of the short batten lies slightly above the S-N curve of the air-box test. Besides, a notable difference was observed in the short and air-box test failure modes, i.e. transverse cracks were observed under the screw head in the air-box tests, but not in the short batten tests (Figures 13 and 15). The reason for the absence of transverse cracks in the short batten tests is considered to be due to the absence of bending action. Therefore, the cantilever batten test was then used to investigate the influence of bending.

The S-N curves of the cantilever and short battens were first compared to investigate the influence of bending on the fatigue pull-through failure (Figure 16). As seen in Figure 16, the roof batten shows a better fatigue performance in short batten tests compared to the cantilever batten tests. It indicates that the fatigue life obtained from the short batten test is always greater than that from the cantilever batten test, which is due to the absence of bending action in the short batten tests. Furthermore, unlike in the short batten tests, cantilever batten tests resulted in transverse cracks under the screw head (Figure 17). This explains the fact that the bending action in the batten induces transverse cracks under the screw heads and thereby influences the fatigue life. Hence, it can be concluded that simulating the bending action is necessary to accurately simulate the fatigue pull-through failure of roof battens. Therefore, short batten tests cannot be considered as the perfect replacement of the air-box test for the fatigue pull-through studies, although it was suitable for the static pull-through studies [9].

As the cantilever batten test eliminates the drawback in short batten test, it was then compared with the air-box test. Figure 18 shows the comparison of S-N curves obtained from the cantilever batten and air-box tests. As seen in Figure 18, fatigue life (number of cycles to failure) from the cantilever batten tests is always less than that obtained from the air-box tests. This indicates that there is another factor, besides bending, that influences the fatigue life. This factor is considered to be the effect of load sharing among supports or screw connections. The nature of load sharing among screw connections (middle and end supports) in a two or more span beam varies with changing connection fixity. This leads to a variation in the reaction forces at the screw connections. This effect in a two-span air-box test can be seen in Figure 19. As seen in this figure, the load transferred to the critical central screw fastener connections in the air-box two-span batten reduces with increasing number of applied load cycles that causes fatigue damage and changes to connection fixity. However, in contrast, the load transferred to the batten to rafter connection in the cantilever batten tests is constant throughout the test as there are no other screw connections to share the load. This is the reason why the fatigue life obtained from the cantilever batten test is always less than the fatigue life obtained from the air-box test. Therefore, a two-span batten test was used to investigate the influence of load sharing effect and to propose a suitable small scale test to replace the full scale air-box test.

Two-span batten test results were first compared with the cantilever batten test results to understand the influence of load sharing among the supports and then compared with the full scale air-box test (Figures 20 and 21). Finally, pull-through failure modes of roof battens (Figure 22) were compared with those observed in the full scale air-box tests (Figure 13). As seen in Figures 20 and 21, the two-span batten test results show a slightly better fatigue performance than the cantilever batten test results, and a good agreement with the air-box test results. It indicates that the differences between the fatigue life obtained from the cantilever batten and air-box (Figure 18) and cantilever batten and two-span batten tests (Figure 20) are due to the effects of load sharing. Also, they reveal that the load transferred to the critical central support of the batten in a two-span batten test reduces with increasing fatigue damage, which enables the batten to survive more cycles compared to the batten in the cantilever batten test where the load transferred to the critical central support is always constant. Similar to the S-N curves, the failure modes of roof battens observed in the two-span batten tests (Figure 22) show a good agreement with the failure modes observed in the full scale air-box tests (Figure 13). In conclusion, although the effects are small, the presence of bending action and load sharing among screw fasteners influence the fatigue life of roof battens. Therefore, it is concluded that the fatigue performance of cold-formed steel roof battens can only be simulated by batten tests with two or more spans. Hence the proposed two-span batten test is the most suitable isolated small scale connection test to simulate the batten performance more precisely in fatigue pull-through studies.

3.3 Crack initiation

In order to study the fatigue behaviour of the roof batten before and after the crack initiation, S-N curves were plotted separately for complete pull-through failure and crack initiation and compared in Figures 23(a) and (b), respectively. According to Figure 23(a), the S-N curves of small scale batten tests plotted for complete pull-through failure slightly deviate from each other and confirm the previous discussion on the effect of bending and load sharing. However, the S-N curves plotted for crack initiation (Figure 23(b)) agree well for all the small scale tests (short, cantilever and two-span). Comparisons of short and cantilever batten test results in Figure 24 and two-span and cantilever batten tests in Figure 25 also further confirm these observations. In Figure 24, the load applied to the critical connection was equally maintained to compare the effect of bending without having the influence of load sharing among screw fasteners. Similarly, in Figure 25, the bending moment at the failure location was equally maintained to compare the effect of load sharing among screw fasteners without having the influence of bending.

As seen in Figure 24, although the S-N curves of short and cantilever batten tests deviate significantly for complete pull-through failure, they agreed well for crack initiation. It leads to an important understanding that the effect of bending on the batten only influences crack growth and not crack initiation. Therefore, considering the finding drawn from the failure mode comparison, i.e. bending action creates transverse crack under the screw head, it can be concluded that the bending action in the roof batten promotes the crack growth in the transverse direction and thereby advances the fatigue pull-through failure. Similarly, although the S-N curves of cantilever and two-span batten tests deviate significantly for complete pull-through failure, they agreed well for crack initiation (Figure 25). It also leads to an important understanding that although load sharing (reduction in central support reaction) commences during early cycles, a significant reduction that affects the batten's behaviour occurs only after the crack initiation, and thereby considerably influences the fatigue life during crack propagation rather than the fatigue life prior to crack initiation. This can also be seen in the load and deflection versus applied load cycles curve (Figure 26), where the load on the critical central support reduces rapidly following crack initiation. This is because of the change in the support condition (stiffness of the batten to rafter connection). The sudden reduction in the critical central support screw tension/reaction force delays the pull-through failure for a certain period, which is unlikely in the short and cantilever batten tests where there is no drop in the critical central support screw tension forces. Similar observations were made by Xu [5] for cladding to batten screw connections.

Based on the above discussions, it is concluded that the absence of load sharing reduces the fatigue life while the absence of bending increases the fatigue life. Therefore, where both bending and load sharing effects are absent, their effects can cancel each other. This is the reason why the S-N curves from the short batten and air-box tests agreed well. Therefore, although the short batten test results agreed well with the air-box test results, the short batten test cannot be used in the fatigue pull-through studies. However, it can be used to predict the fatigue life up to crack initiation. On the other hand, the cantilever batten test could be used in the fatigue life prediction studies in terms of crack initiation and complete pull-through failure as it yields conservative test results (Figure 25). Overall, considering the load sharing effect, it is recommended that the small scale two-span batten test is the suitable test method to conduct the fatigue pull-through failure studies of CFS roof battens.

4 FATIGUE DESIGN METHOD

In this section, the test results of two-span batten tests were used to determine the fatigue capacity of G550-0.75 roof battens. Initially, the fatigue pull-through capacity was determined in terms of the endurance limit using the S-N curves developed from the constant amplitude cyclic tests. Figure 27 shows the S-N curves developed for crack initiation and complete pull-through failure from the two-span batten tests. As seen in Figure 27, the S-N curves for crack initiation and complete pull-through failure illustrate the increment in fatigue life with decreasing cyclic load magnitude. It can be noted that for the cyclic load range (maximum cyclic load) below 50% SPC, fatigue life increases rapidly. This indicates the presence of the endurance limit to be closer to 40% SPC. Therefore, 40% SPC can be safely taken as the fatigue capacity of G550-0.75 battens.

However, for the 40% cyclic load, the roof batten will survive a minimum of about 24,000 cycles (Figure 27). Such a long exposure period with a large cyclic load magnitude (40% SPC) is unlikely for a typical steel roof in a cyclone. Therefore, using the endurance limit of 40% SPC may be too conservative. According to the NCC [12], cyclone impact on a building roof can be simulated by the LHL loading sequence consisting of about 10,000 cycles. Therefore, an alternate approach was proposed to determine the fatigue capacity based on the number of cycles. For instance, the fatigue capacity of the roof batten considering 10,000 cycles is 50% SPC (Figure 27). The same can be taken as 45% to design the batten free from cracks (Figure 27). These capacity reductions due to cyclic wind uplift loading can be directly obtained from the S-N curves developed from small scale two-span batten tests (Figure 27). In order to determine the capacity reduction (R_f), simple equations were developed for both crack initiation and complete pull-through failure using the experimental data and are presented as Equations 1 and 2, respectively.

$R_f = 1 - 0.6\,(1 - e^{-0.0002\,x})$ for complete pull-through failure (N_f) (1)

$R_f = 1 - 0.6\,(1 - e^{-0.0003\,x})$ for crack initiation (N_i) (2)

where, x - Number of cycles for a design wind event

This fatigue capacity reduction factor, R_f, was then included in the recently developed static pull-through capacity equation for high strength cold-formed steel roof battens [10, 11]. This enables the equation to be adopted as a standard pull-through equation suitable for both static and cyclic wind load conditions. The modified pull-through design equation is shown in Equation 3.

$$\phi \; F_{ov} = \phi \; 8.68 \; R_f \; t^2 \; f_u \qquad (3)$$

where, F_{ov} - Pull-through capacity in Newtons

ϕ - Capacity reduction factor = 0.6

R_f - Reduction factor for fatigue design

t - Steel thickness in contact with the screw head

f_u - Measured ultimate tensile strength of the batten material

The reduction factor, R_f, is equal to one for static pull-through designs. For fatigue designs, it can be taken as 0.4 (endurance limit approach) to conservatively design the roof battens for fatigue pull-through failures regardless of the number of cycles. Alternatively, Equations 1 and 2 can be used to predict the fatigue capacities for varying design wind events or fatigue life requirements. This equation only gives the static and fatigue pull-through capacities of roof battens. However, in the real wind case, ultimate roof failure may be due to other failures such as pull-out and member failures. Also, such failures may occur in some other members or connections such as cladding to batten. So, when designing roofs, all possible failures must be considered and design for the critical failure.

It must be noted that the S-N curves and the design equation were developed by only considering the tests of G550-0.75 roof battens. However, the same procedure can be followed to design other roof battens made of different steel grades and thicknesses. Also, it should be noted that the real cyclone wind loading is not a constant amplitude type. Therefore, a similar design method, but considering the realistic multi-level cyclic loading such as that simulated by LHL cyclic load sequence, is preferred. This study establishes a foundation for developing such an optimised design method.

5 CONCLUSIONS

This paper has presented the details of developing a simple, small scale test method to conduct the fatigue pull-through studies of cold-formed steel roof battens, and a simple fatigue design equation developed using the selected small scale constant amplitude cyclic test method. Following conclusions have been drawn from this study:

- Despite the fact that the full scale air-box test is the closest representation of the actual roof assembly and suitable for simulating the effects of cyclonic wind actions, it is not the preferred test method for connection studies due to the difficulties, time and cost associated with such full scale tests.
- The short batten test method recommended for static pull-through studies cannot be used in fatigue pull-through studies as they do not simulate the bending action, which influences the fatigue life of roof battens.
- Roof battens with at least two spans is necessary to conduct the fatigue pull-through tests as load sharing among the screw fasteners in adjacent supports influences the fatigue life.
- The effects of bending action and load sharing influence the fatigue behaviour of roof battens only during crack propagation and not prior to crack initiation.
- A small scale two-span batten test without cladding and cladding to batten screw connections can be used satisfactorily to study the fatigue pull-through behaviour of roof battens. This makes the experiments less time consuming, economical and simpler than those based on full scale air-box tests.
- Fatigue pull-through capacity of the industrial G550-0.75 roof batten can be conservatively taken as 40% of the static pull-through capacity. Alternatively, Equations 1 to 3 can be used to predict the fatigue pull-through capacities depending on the loading cycles in a design wind event.

ACKNOWLEDGEMENTS

The financial support of the Australian Research Council (Grant Number DP120103366) and Queensland University of Technology (QUT), as well as the contribution of the technical staff in QUT's O-block laboratory and Banyo Pilot Plant Precinct is gratefully acknowledged.

REFERENCES

[1] Beck VR. Appraisal of roof cladding under dynamic wind loading – Cyclone Tracy Darwin, 1974. Technical report No. 1, Housing Research Branch, Department of Housing and Construction, Melbourne, Australia.1975.

[2] Morgan J, Beck VR. Failure of Sheet-metal Roofing Under Repeated Wind Loading. Barton, Australia: Institution of Engineers, Australia; 1976. p. 290-4.

[3] Baskaran A, Molleti S, Roodvoets D. Understanding Low-Sloped Roofs Under Hurricane Charley From Field to Practice. Journal of ASTM International. 2007;4:1-13.

[4] Mahendran M. Fatigue behaviour of corrugated roofing under cyclic wind loading. Civil Engineering Transactions, Institution of Engineers Australia. 1990;32:212-8.

[5] Xu YL. Fatigue Performance of Screw-Fastened Light-Gauge-Steel Roofing Sheets. Journal of Structural Engineering. 1995;121:389-98.

[6] Xu YL. Determination of Wind-Induced Fatigue Loading on Roof Cladding. Journal of Engineering Mechanics. 1995;121:956-63.

[7] Boughton GN, Falck DJ. Tropical Cyclone George damage to buildings in the Port Hedland area. Technical Report 52, Cyclone Testing Station, James Cook University, Townsville, Australia.2007.

[8] Ginger JD. Characteristics of wind loads on roof cladding and fixings. Wind and Structures, An International Journal. 2001;4:73-84.

[9] Sivapathasundaram M, Mahendran M. Development of Suitable Test Methods for the Screw Connections in Cold-Formed Steel Roof Battens. Journal of Structural Engineering. 2016;142:4016025.

[10] Sivapathasundaram M, Mahendran M. Experimental studies of thin-walled steel roof battens subject to pull-through failures. Engineering Structures. 2016;113:388-406.

[11] Sivapathasundaram M, Mahendran M. Numerical Studies and Design of Thin Steel Roof Battens Subject to Pull-through Failures. Engineering Structures (under review). 2017.

[12] Australian Building Codes Board. National Construction Code: Class 1 & 10 buildings. Canberra, Australia; 2015.

[13] Mahendran M. Towards an appropriate fatigue loading sequence for roof claddings in cyclone prone area. Engineering Structures. 1995;17:476-84.

[14] Beck VR, Stevens LK. Wind loading failures of corrugated roof cladding. Civil Engineering Transactions, Institution of Engineers Australia. 1979;21:45-56.

[15] Mahendran M, Mahaarachchi D. Cyclic Pull-Out Strength of Screwed Connections in Steel Roof and Wall Cladding Systems using Thin Steel Battens. Journal of Structural Engineering. 2002;128:771-8.

[16] Standards Australia. AS 4040.3: Methods of testing Sheet Roof and Wall Cladding - Resistance to Wind Pressures for Cyclone Regions. Sydney, Australia; 1992.

[17] BlueScope Steel Limited. Design and installation guide for building professionals. Industrial catalogue, Australia; 2014.

[18] American Iron and Steel Institute. AISI S905: Test Methods for Mechanically Fastened Cold-formed Steel Connections. Washington, DC, USA; 2008.
[19] Lovisa AC, Henderson DJ, Ginger JD, Walker G. Characterising fatigue macrocrack initiation in profiled steel roof cladding. Engineering Structures. 2016;125:364-73.
[20] Mahendran M. Behaviour and design of crest-fixed profiled steel roof claddings under wind uplift. Engineering Structures. 1994;16:368-76.
[21] Huh H, Lim JH, Park SH. High speed tensile test of steel sheets for the stress-strain curve at the intermediate strain rate. International Journal of Automotive Technology. 2009;10:195-204.
[22] Yu WW, Kassar M. Effect of Strain Rate on Material Properties of Sheet Steels. Journal of Structural Engineering. 1992;118:3136-50.
[23] Gray GT. High-Strain-Rate Deformation: Mechanical Behavior and Deformation Substructures Induced. Annual Review of Materials Research. 2012;42:285-303.

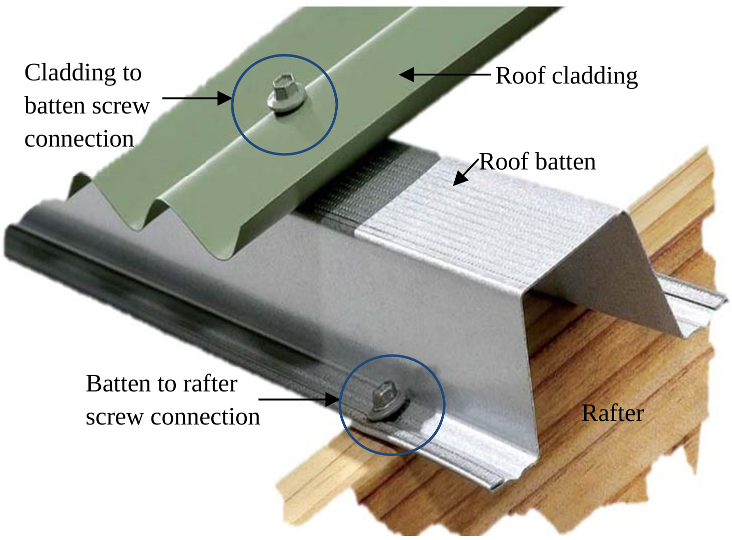

Figure 1: Typical roof connections

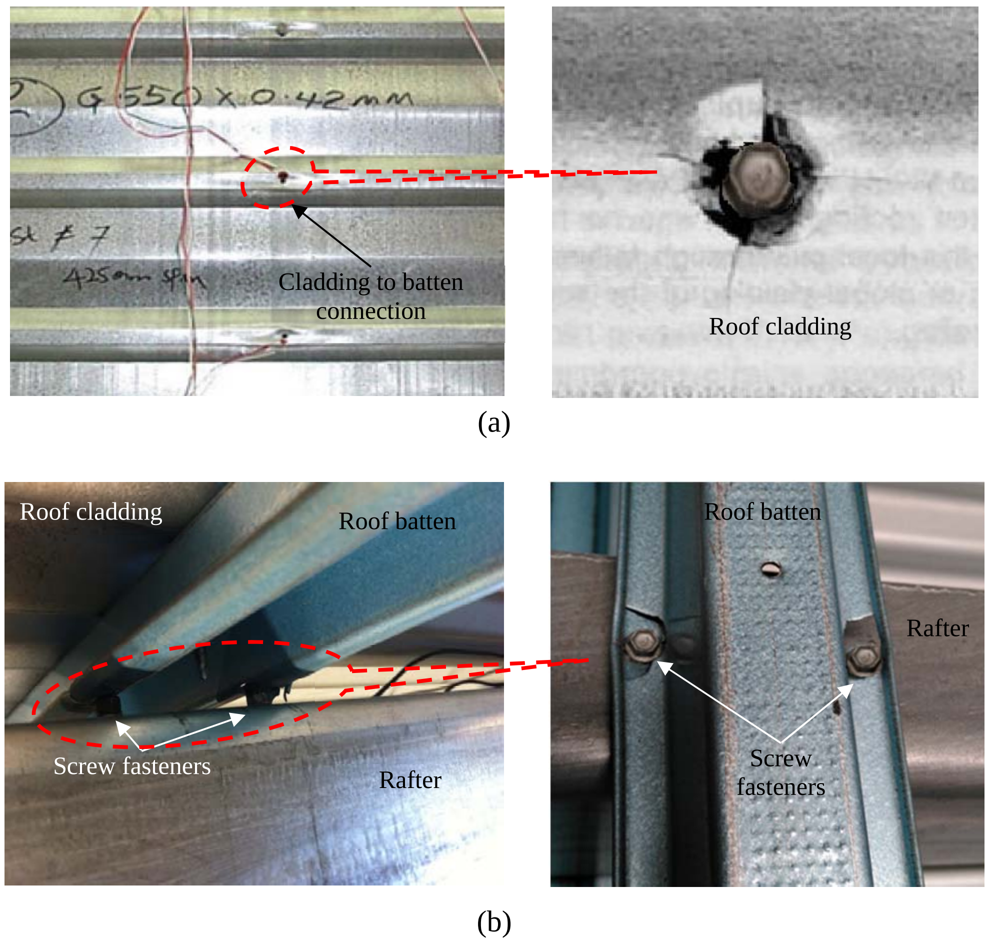

Figure 2: Pull-through failures: (a) Cladding to batten connection [15]; (b) Batten to rafter connection

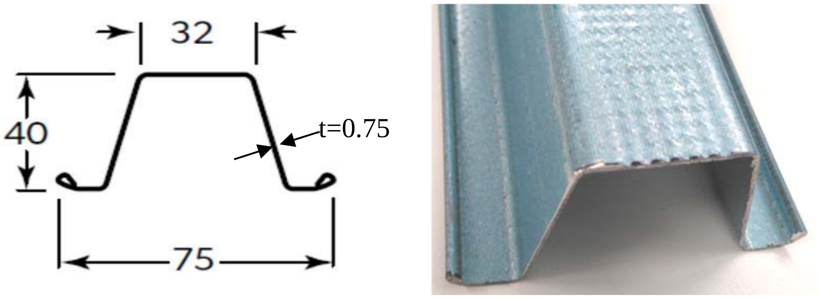

Figure 3: Test roof batten

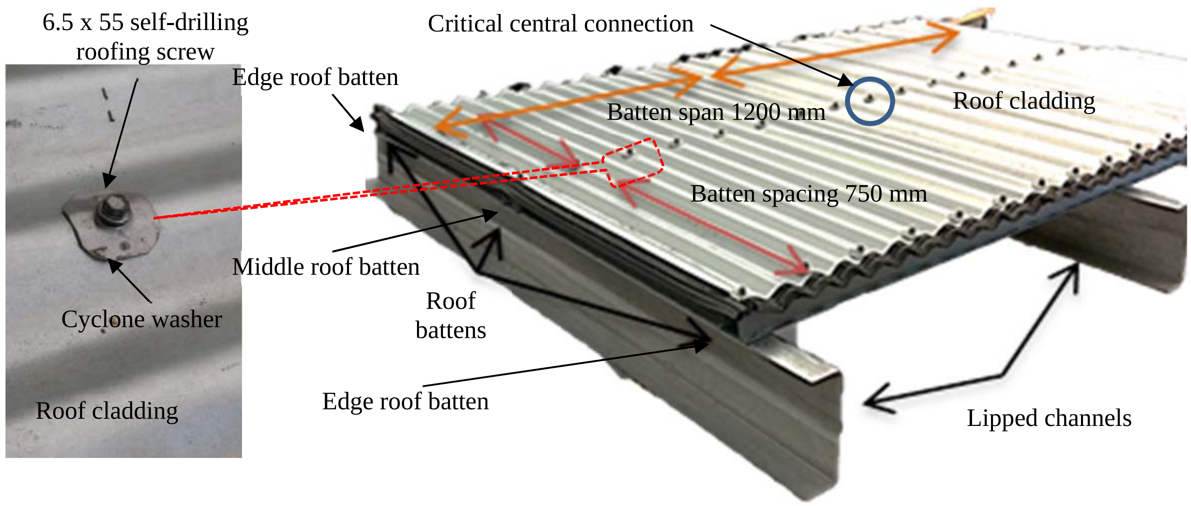

(a)

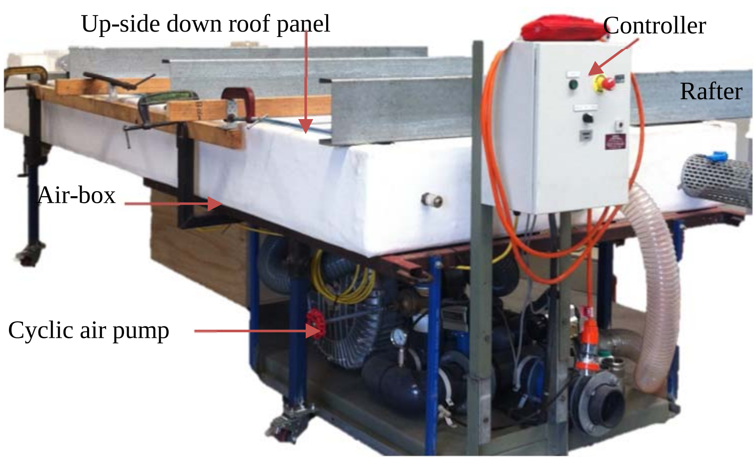

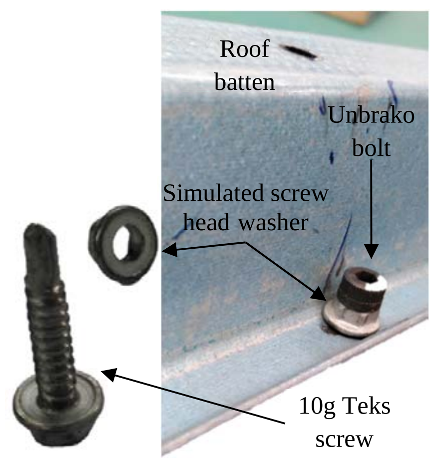

(b) (c)

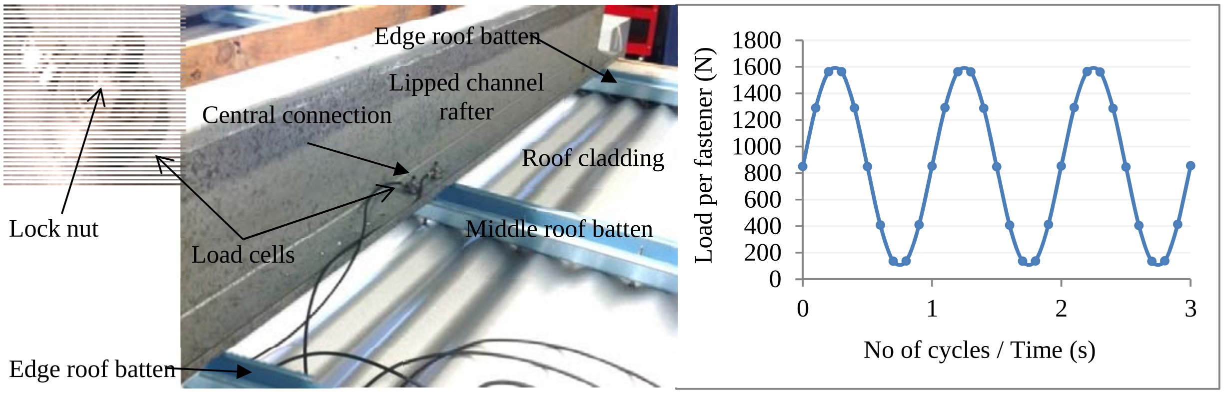

(d) (e)

Figure 4: Full scale two-span roof test: (a) Roof assembly; (b) Test set-up; (c) Simulated screw connection; (d) Individual fastener reaction measurement using washer load cells; (e) Variation of load per fastener in a 50% cyclic test

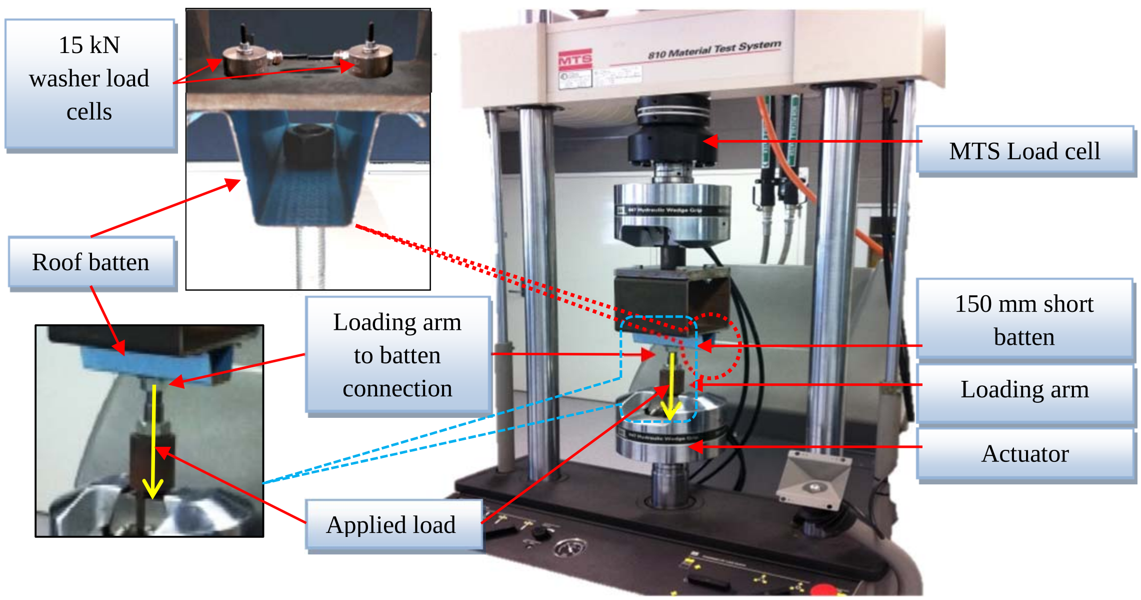

Figure 5: Short batten test

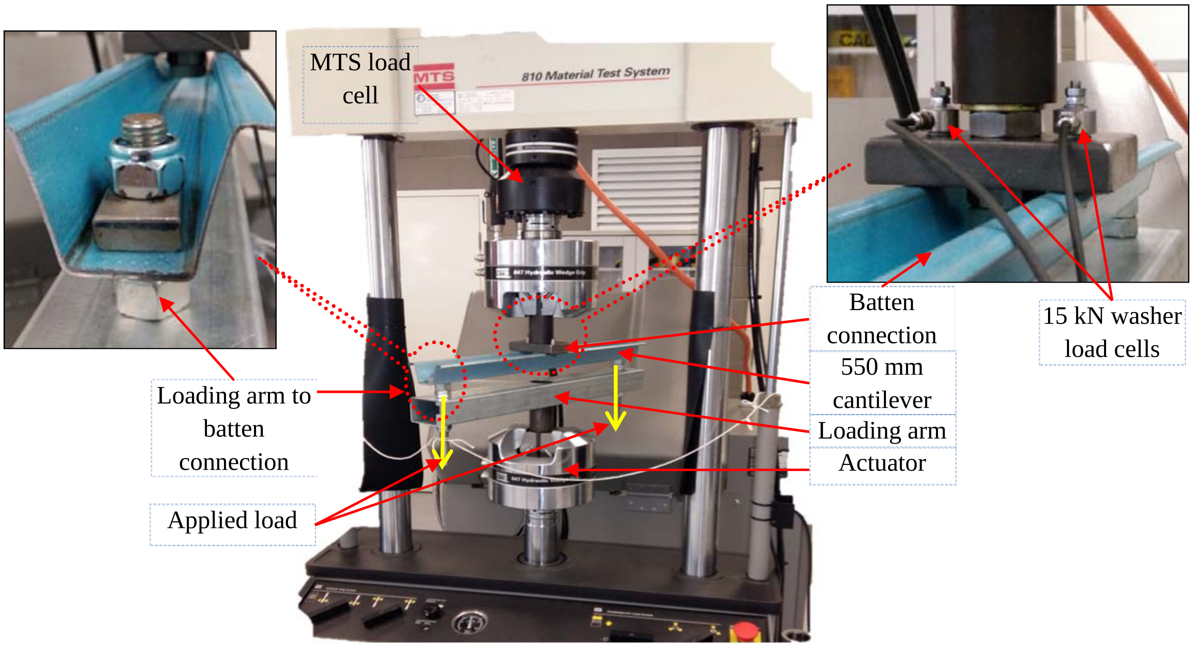

Figure 6: Cantilever batten test

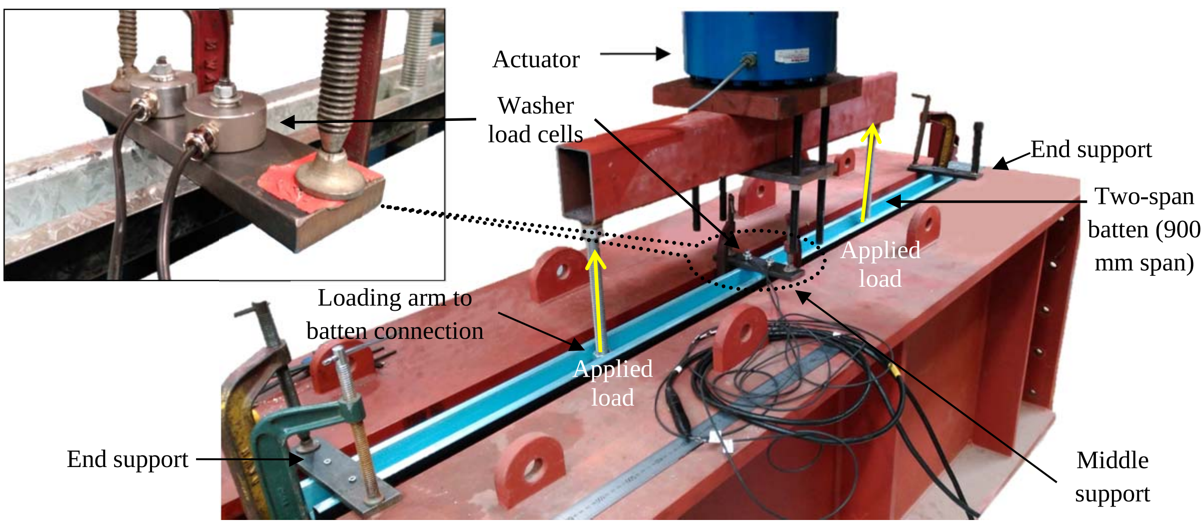

Figure 7: Small scale two-span batten test

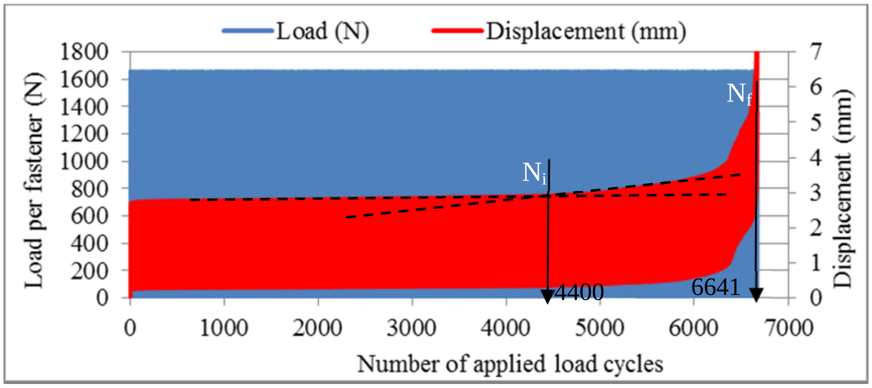

Figure 8: Determining N_i from a 58% cyclic test

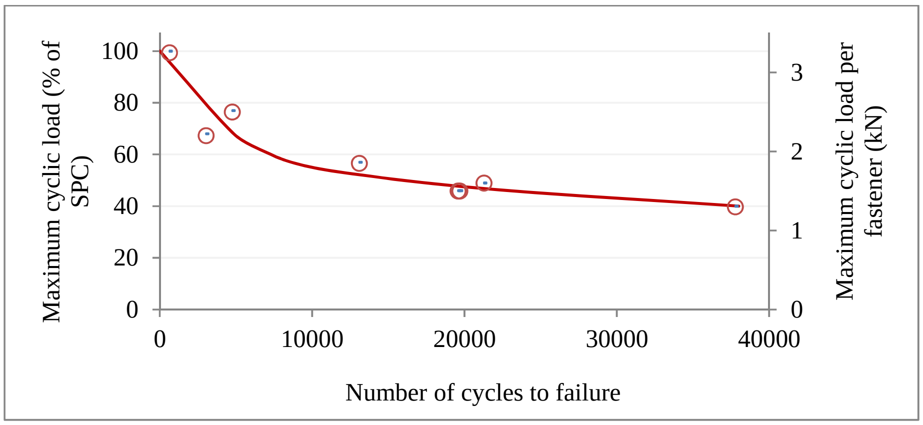

Figure 9: S-N curve from full scale air-box tests

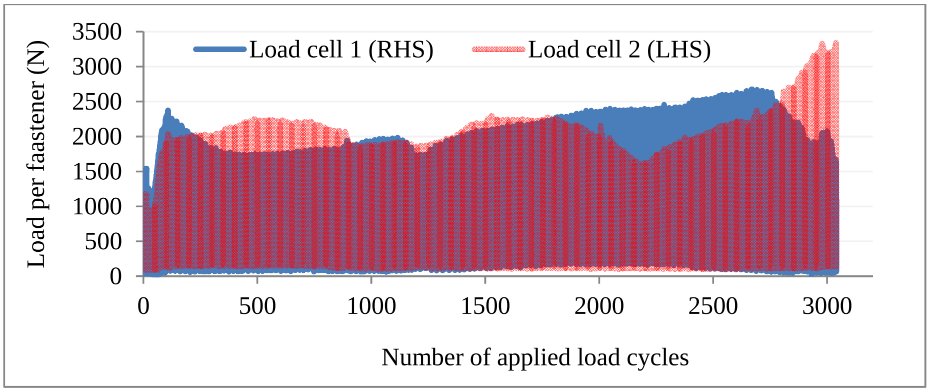

Figure 10: Fastener reaction versus number of applied load cycles curves of 68% cyclic test (full scale air-box Test A-3)

(a)

(b)

Figure 11: Importance of correct screw fastening: (a) Poor cladding to batten screw fastening; (b) Perfect cladding to batten screw fastening

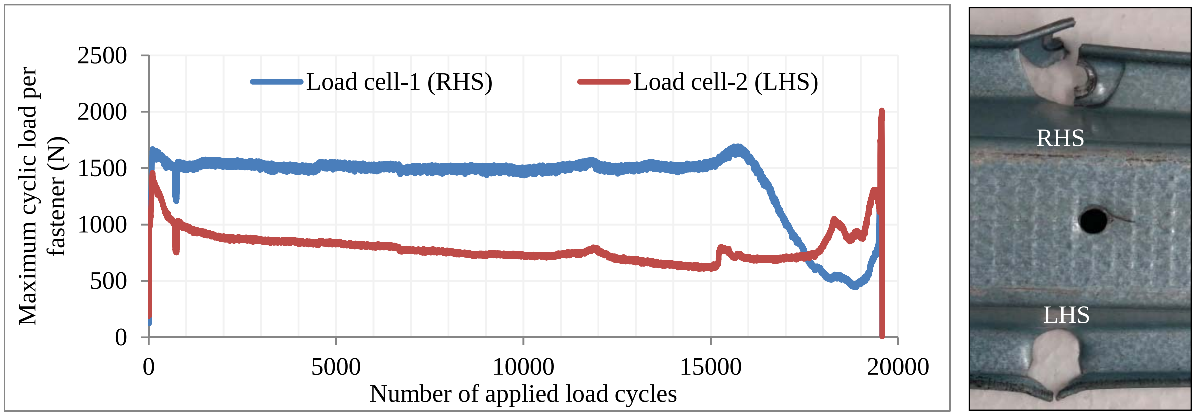

(a) (b)

Figure 12: Typical unequal load distribution in an air-box cyclic test: (a) Maximum cyclic load per fastener versus number of applied load cycles curves; (b) Failure modes

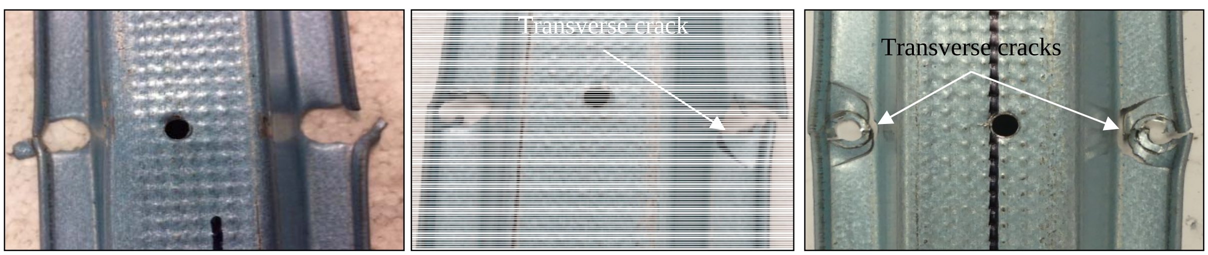

(a) Static test (b) 100% Cyclic test (c) 77% Cyclic test

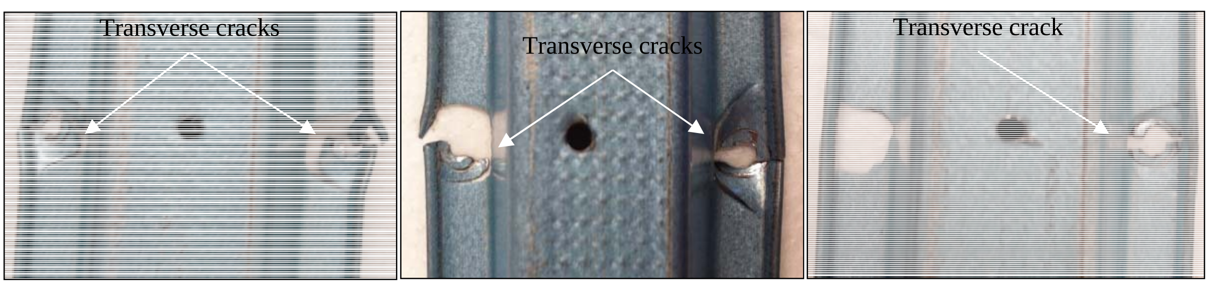

(d) 68% Cyclic test (e) 57% Cyclic test (f) 49% Cyclic test

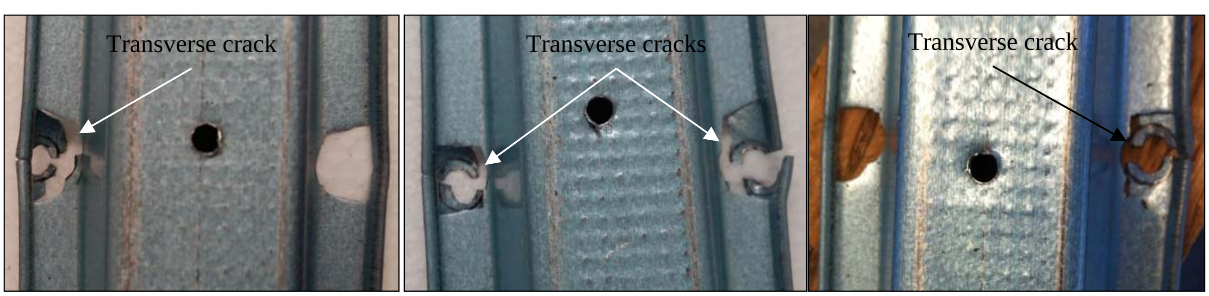

(g) 46% - 1 Cyclic test (h) 46% - 2 Cyclic test (i) 40% Cyclic test

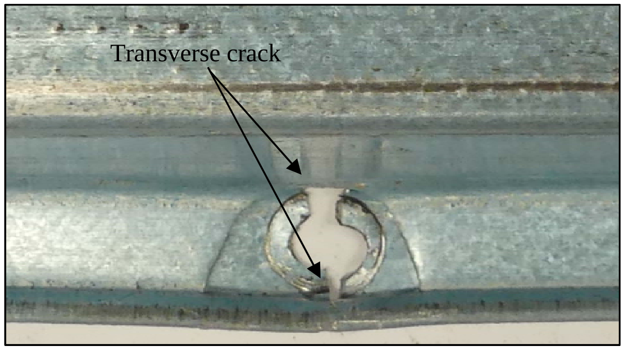

(j) Typical transverse crack

Figure 13: Failure modes observed in the full scale air-box tests

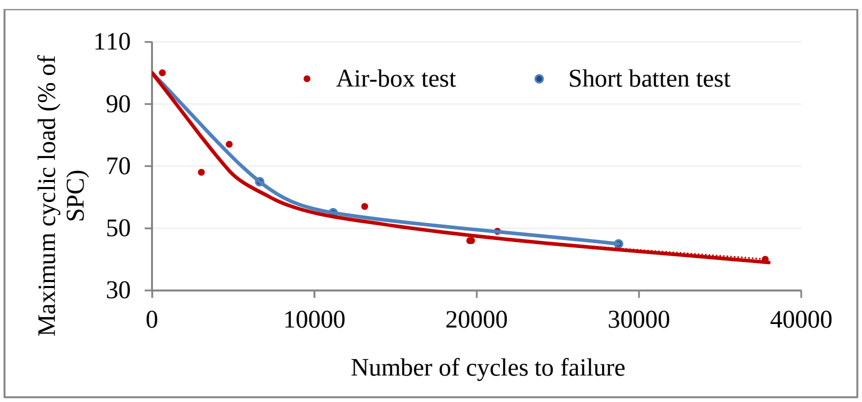

Figure 14: S-N curves of G550-0.75 roof battens from air-box and short batten tests for complete pull-through failure

(a) Static test

(b) 66.6% Cyclic test

(c) 56.3% Cyclic test

(d) 46.1% Cyclic test

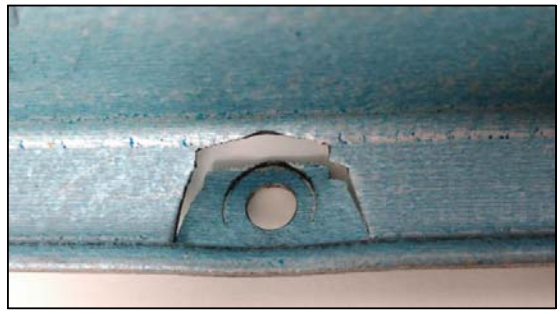

(e) No transverse crack

Figure 15: Failure modes observed in the short batten tests

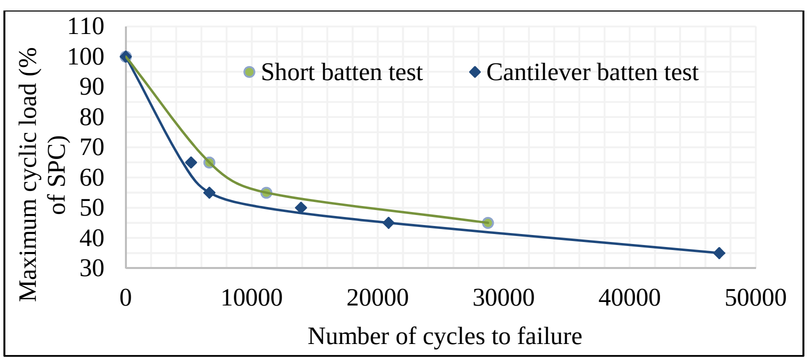

Figure 16: S-N curves from cantilever and short batten tests for complete pull-through failure

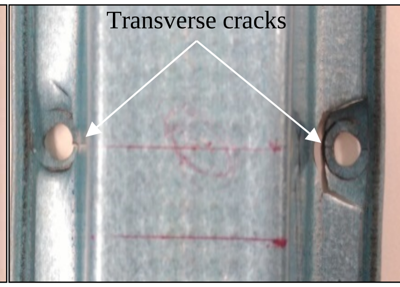

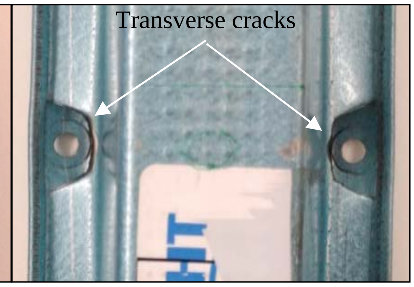

(a) Static test (b) 68.4% Cyclic test (c) 57.9% Cyclic test

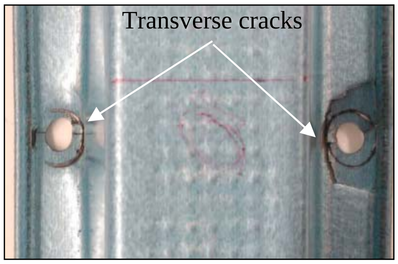

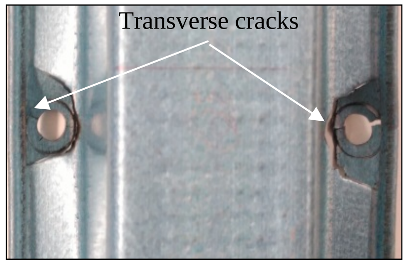

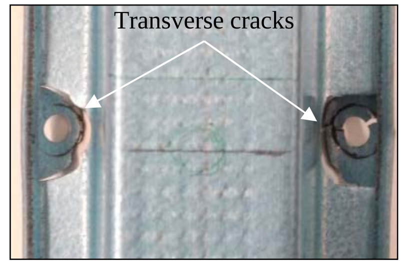

(d) 52.6% Cyclic test (e) 47.4% Cyclic test (f) 36.8% Cyclic test

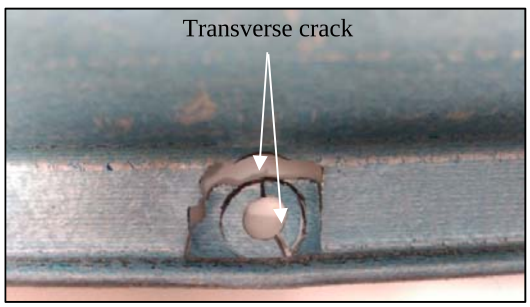

(g) Transverse crack

Figure 17: Failure modes observed in the cantilever batten tests

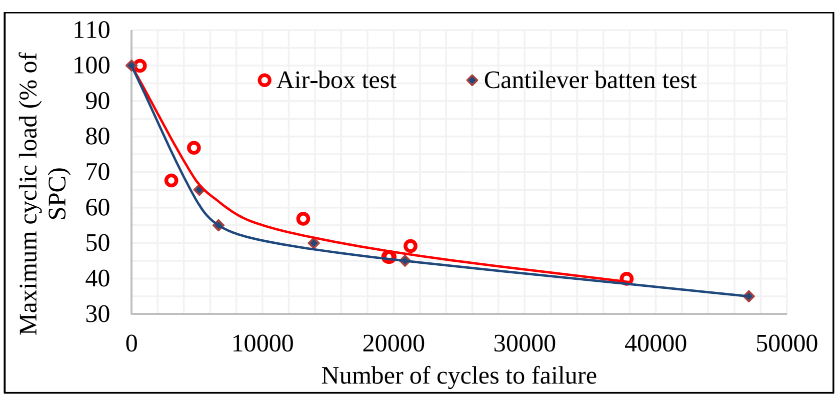

Figure 18: S-N curves from air-box and cantilever batten tests for complete pull-through failure

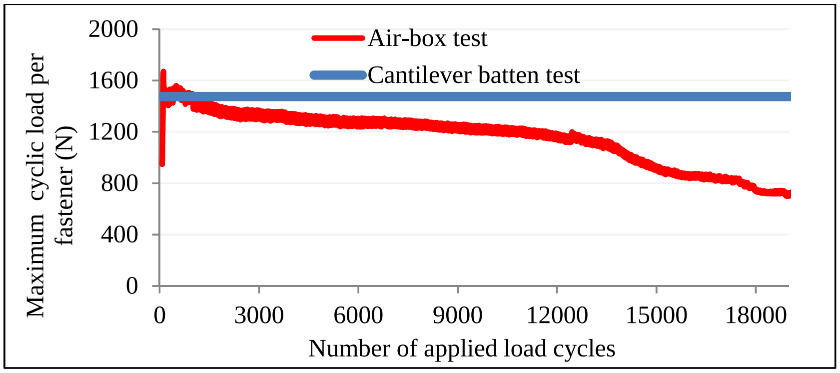

Figure 19: Comparison of maximum cyclic load per fastener variations in air-box and cantilever batten tests (46% cyclic load)

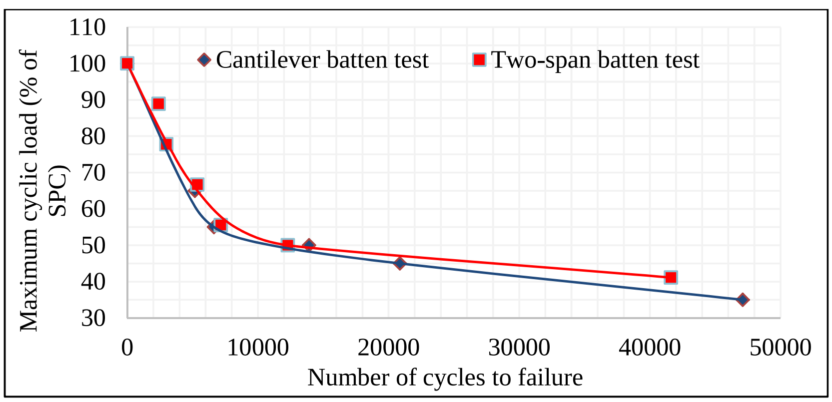

Figure 20: S-N curves from cantilever and two-span tests for complete pull-through failure

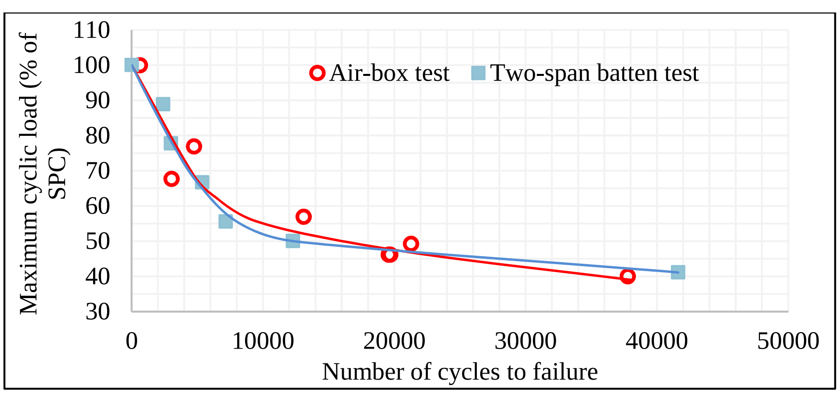

Figure 21: S-N curves from air-box and two-span batten tests for complete pull-through failure

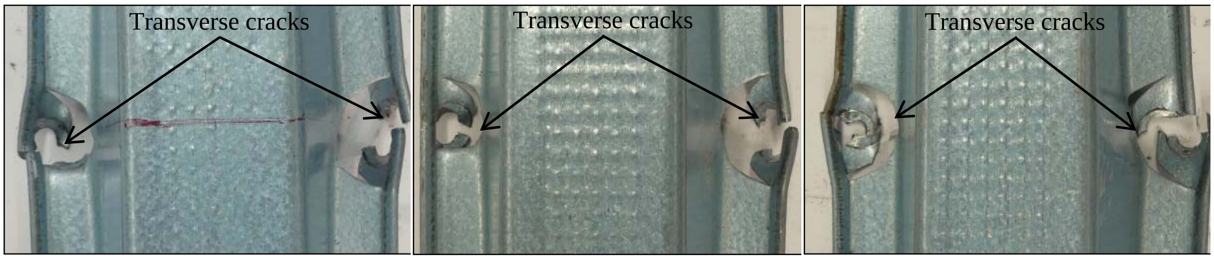

(a) 89% Cyclic test (b) 78% Cyclic test (c) 67% Cyclic test

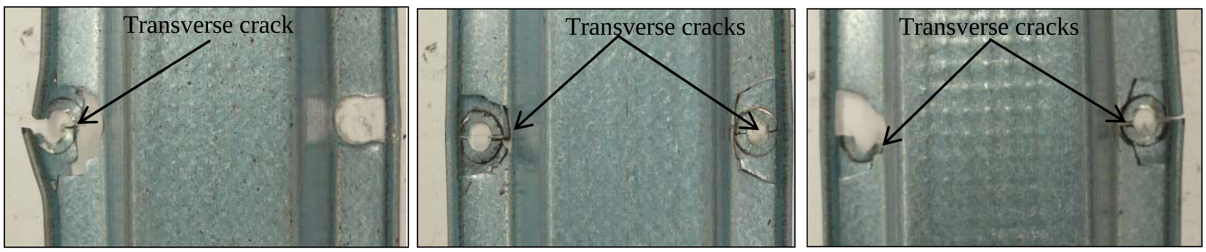

(d) 56% Cyclic test (e) 50% Cyclic test (f) 41% Cyclic test

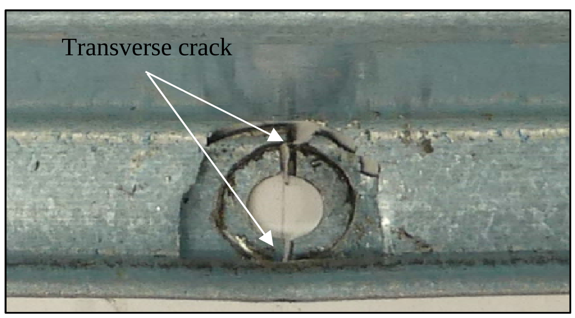

(g) Transverse crack

Figure 22: Failure modes observed in the two-span batten tests

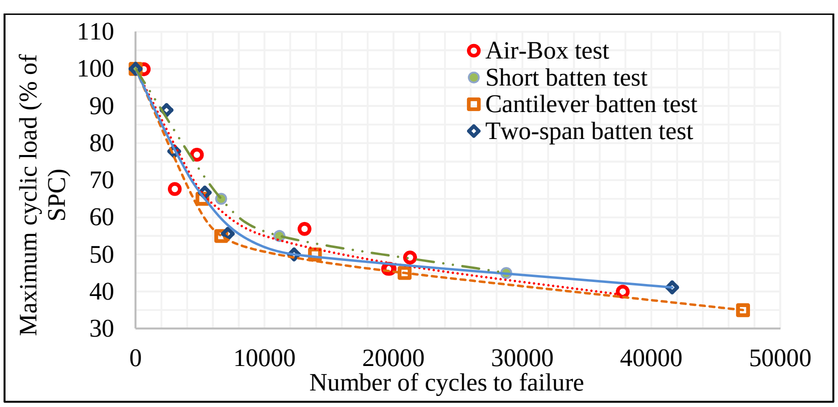

(a)

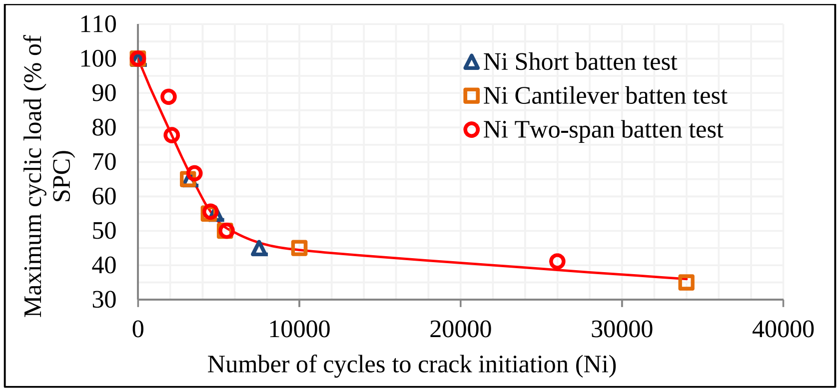

(b)

Figure 23: S-N curves for: (a) Complete pull-through failure; (b) Crack initiation

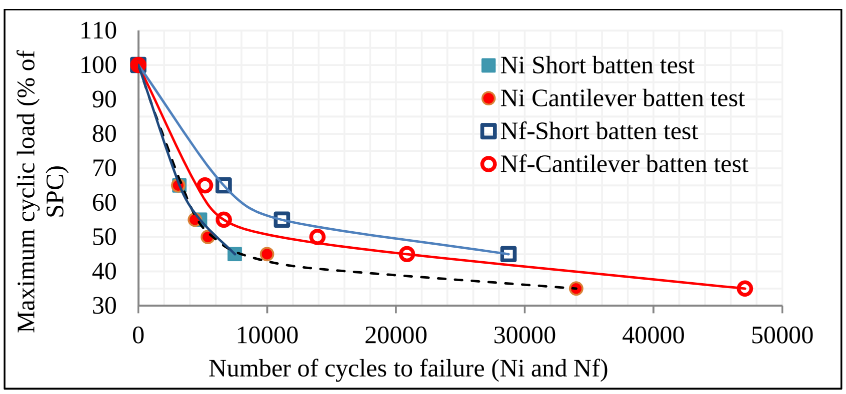

Figure 24: S-N curves from short and cantilever batten tests for crack initiation and complete pull-through failure

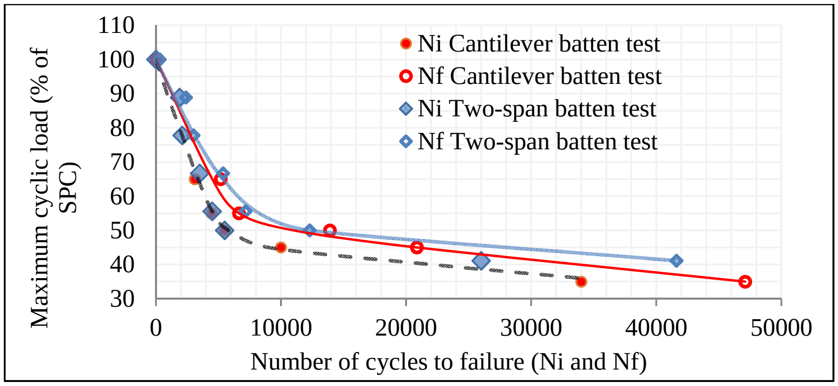

Figure 25: S-N curves from cantilever and small scale two-span batten tests for crack initiation and complete pull-through failure

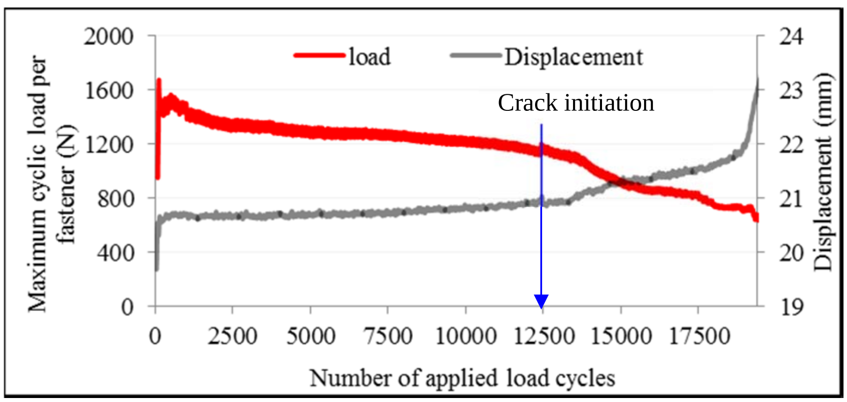

Figure 26: Variation in central support reaction with increasing load cycles in a 46% cyclic test

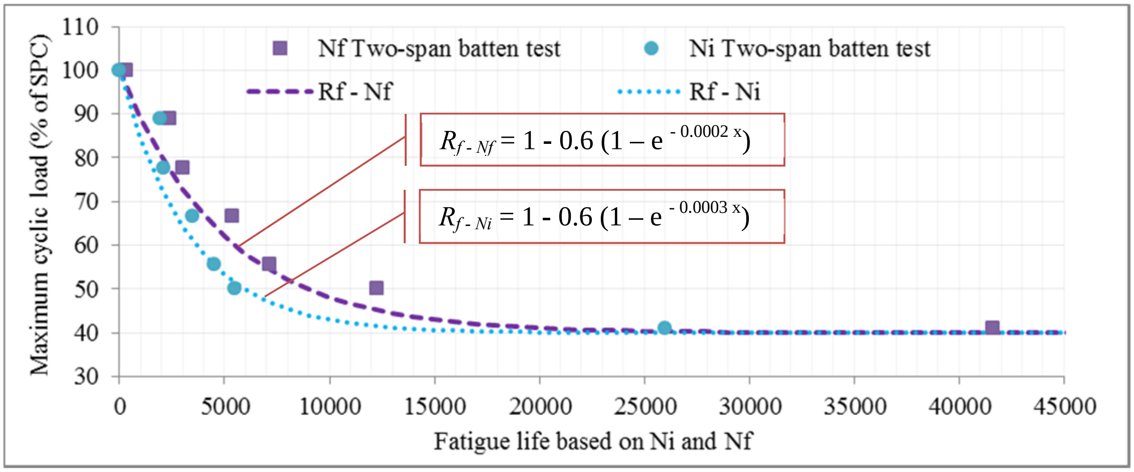

Figure 27: Proposed reduction factor R_f

Table 1: Static pull-through capacities of G550-0.75 roof battens

Test	Static Capacity per fastener (kN)	Mean	COV
Air box test	3.06, 3.09, 3.61	3.25	0.10
Short batten test	2.79, 2.94, 2.96, 3.01	2.93	0.03
Cantilever batten test	2.76, 2.71, 2.93, 2.98	2.85	0.05
Two-span batten test	3.00, 3.10, 3.12	3.07	0.02

Table 2: Cyclic test results of G550-0.75 roof battens from full scale air box tests

Test No	Max. cyclic load per fastener (kN)	Max. cyclic load (% of SPC)	Number of cycles to failure
A-1	3.25	100	635
A-2	2.50	77	4753
A-3	2.20	68	3041
A-4	1.85	57	13100
A-5	1.60	49	21280
A-6	1.50	46	19581
A-7	1.50	46	19692
A-8	1.30	40	37781

Table 3: Cyclic test results of G550-0.75 roof battens from two-span batten tests

Test No	Max. cyclic load per fastener (kN)	Max. cyclic load (% of SPC)	Number of cycles to failure	
			N_i	N_f
T-1	3.07	100	280	308
T-2	2.73	89	1900	2400
T-3	2.39	78	2100	3000
T-4	2.05	67	3500	5372
T-5	1.71	56	4500	7162
T-6	1.54	50	5500	12290
T-7	1.26	41	26000	41617

Table 4: Cyclic test results of G550-0.75 roof battens from cantilever batten tests

Test No	Max. cyclic load per fastener (kN)	Max. cyclic load (% of SPC)	Number of cycles to failure	
			N_i	N_f
C-1	1.95	68.4	3100	5179
C-2	1.65	57.9	4400	6641
C-3	1.50	52.6	5400	13909
C-4	1.35	47.4	10000	20866
C-5	1.05	36.8	34000	47107

Table 5: Cyclic test results of G550-0.75 roof battens from short batten tests

Test No	Max. cyclic load per fastener (kN)	Max. cyclic load (% of SPC)	Number of cycles to failure	
			N_i	N_f
S-1	1.95	66.6	3200	6633
S-2	1.65	56.3	4800	11153
S-3	1.35	46.1	7500	28745